

# Design and Analysis of an Orthotic Device with Torque Reducing Mechanism for Knee Joint during Normal Walking

Abhishek Rudra Pal<sup>1</sup>, Dilip Kumar Pratihar<sup>2</sup> (corresponding author), Sanjay Gupta<sup>3</sup>

<sup>1</sup>Advanced Technology and Development Center

<sup>2,3</sup>Department of Mechanical Engineering

Indian Institute of Technology Kharagpur

Kharagpur -721302, West Bengal, India

Email: <sup>1</sup>abhishekrudrapal@gmail.com, <sup>2</sup>dkpra@mech.iitkgp.ernet.in, <sup>3</sup>sangupta@mech.iitkgp.ernet.in

**Abstract**—An orthotic device is used to assist movements of the patients having physical disabilities. The objectives of this study are to develop an analytical model of kinematics and dynamics of human walking, and to design an external orthotic device for assisting patients with impairment at knee joint. A mechanism is incorporated with this device, which will reduce the knee joint torque during walking. The values of knee joint torque and power consumption are determined for two cases, with and without the torque reducing mechanism. Results have been verified using solid-works. For maintaining the stability of the human body while walking, loci of Zero Moment Point and Dynamic Balance Margin are also obtained. For the orthotic device with mechanism, a reduction of 92% in maximum torque is obtained in comparison to the device without any such mechanism. Thus, a novel design of an optimized orthotic device has been obtained with the above torque reducing mechanism.

**Keywords**— orthotic device; knee joint; zero moment point; dynamic balancing margin; real coded-Genetic Algorithm.

## I. INTRODUCTION

Considering the demography [1] of older individuals, it is found that during 1950s only 4.9% of the world's population was over the age of 65. In 2007, almost 20% of world's population was over 65. According to World Health Organization [2], the world's population of people within the age group of 60 years and above, has been doubled since 1980. It has been predicted to reach 2 billion by 2050 that will be approximately 35% of the total population. Rehabilitation robotics plays an important role in taking care of older people to regain their physical activity. Application of rehabilitation robotics is not only limited for serving patients of older age but they can also be used by patients, who are suffering from motor impairment due to neurological disorder. These robotic devices can also be utilized in military applications to help soldiers, who have lost their limbs in wars. There are primarily two types of rehabilitation robotic devices, namely prosthetic device (prosthesis) and orthotic device (orthosis). In prosthesis [3], the individual's missing limbs are replaced by artificial parts or devices that usually replicate the motion exerted by original limbs. However, the patients who are

suffering from different spinal cord injuries or stroke, orthotic devices (can be called as Orthoses) are used. Orthoses [4] are artificial instrument to support the skeletal system to modify proper functional characteristics of neuromuscular activity. The patients for whom, recovery is possible, these devices may be used by physiotherapist to restore the limb's original movement by proper training of patients with the device. The patients for whom, recovery is not possible, this device can be used as a permanent support.

The increase in number of older people or motor impaired patients indicates a large demand for orthotic devices. Although there exist a number of orthotic devices developed by several researchers throughout the world, the majority of them are in prototype or laboratory stage. Moreover, higher cost of fabrication of these devices makes them unaffordable to common people for use. There is a scarcity of development of such devices based on human gait cycle. This paper is focused on design and development of such an orthotic device based on the kinematics and dynamics of the human gait cycle. Design of the orthotic device is also attempted by considering cost effectiveness and suitability of use for patients.

## II. LITERATURE REVIEW

Bradley et al. [5] designed a robotic device, which helped physiotherapists to manipulate the patient's limb to return their activities. A patient used to insert his/her legs into the provision attached with these devices and then with the actuator's motion, his/her leg could be moved according to physiotherapist's instruction. However, no attempt was made to develop adaptive controller in order to meet the patient's and physiotherapist's requirement. Safizadeh et al. [6] presented a work on kinematic analysis of lower limb orthotic device for both knee and hip joints using a single DC motor. The knee motion was controlled by a cam profile generated based on joint angles provided by kinematic analysis of human walking. But, no dynamic analysis and experiment had been carried out with the proposed device worn by patients. Zhang, Tian and Guo [7] designed a passive lower limb exoskeleton, which was accompanied by an omni-

directional vehicle in order to enable the patients to move in all directions. The main purpose of that device was to reduce physical cost of patient by selecting the design parameters through an optimization to get minimum power consumption. This device assisted spinal cord injury patients for swing phase only. No mechanism was incorporated for stance phase. Agrawal et al. [8] designed a gravity balanced passive orthotic device, where no motor was used as power source. The unloading of limb was achieved through gravity load within its range of motion. Here, the device was used to get different levels of assistance starting from 0% to 100%, according to the patient's need. This exoskeleton was used by patients to recover normal locomotion through training but could not be used by the patients who needed permanent assistance. Yamamoto, Ishii, Hyodo, Yoshimitsu and Matsuo [9] developed an orthotic device to assist nurses to transfer patients, where pneumatic rotary actuators were used for knee flexion/extension. The method of attachment adopted for this device with user and nature of unactuated joints were not mentioned in this work. Lemaire, Goudreau and Yakimovich [10] presented an orthotic device, where the driving unit was a rotary hydraulic mechanism. The basic principle lies on the fact that knee flexion velocity was more during knee-collapse event than that during walking. Its operation was based on the valve and spring mechanisms, used to control the flow in the device. The scarcity of detailed understanding of position and time of knee engagement during walking or stumble were the major drawbacks of this device. Nikitzuk, Weinberg, Canavan and Mavroidis [11], designed a novel orthotic device which was capable to provide variable damping at knee joint. Electrorheological fluid was used in the brake. By varying the electric field, the fluid's viscosity could also be varied to provide different torques. This device was not tested with the patients during real walking.

From all the above studies, it is found that there had been an inadequacy of generalized modelling of human walking dynamics. Moreover, most of the devices that had been developed were of high cost and tested in treadmill instead of real walking.

In the present article, a model of human's lower extremity along with the upper one (refer to Fig. 1) is drawn using solid-works. Thigh and shank of the model are inserted into their respective braces. The values of the masses of different limbs of this model are assumed to be larger than that of the original limbs of an average human being to ensure a safe design. The ranges of joint angles are taken lower than that required for the normal walking, as the patient cannot move his/her limbs like a normal humans. Then, dynamic study is conducted using solid works to find out the values of the torque and power consumption. Now, the expressions for both torque and power consumption at knee joint are determined analytically using Lagrangian approach. Then, Zero Moment Point (ZMP) and Dynamic Balance Margin (DBM) are also calculated according to the change of position of foot polygon with time. A mechanism is incorporated, which is attached to the device in order to reduce the torque. Genetic Algorithm (GA) is used to get the minimum torque value at knee joint, with the condition that DBM of the system is maintained.

Therefore, the aim of this study is to design an optimal orthotic device with a suitable torque reducing, geared four-bar mechanism

### III. THEORITICAL FORMULATION

#### A. Device Without Mechanism

In Fig. 1(a), different parts of lower limb are shown, where the part HAT denotes the combination of Head, Arms and Trunk, because these three parts are assumed to act like a single part for the sake of simplicity of analytical modeling. An elliptical metal belt of light weight is attached with the waist of patient. The belt's thickness and height are taken to be equal to 4.0 mm and 40.0 mm, respectively. The lengths of major and minor axes of the elliptical belt are considered as 170.0 mm and 120.0 mm, respectively. Thigh and shank of both the legs are attached with hollow cylindrical braces (denoted as thigh and shank holders) having the dimensions, approximately same to those of an average human being. Inner radii of thigh and shank holders are assumed to be equal to 108.0 mm and 68.0 mm, respectively. Height and thickness are taken to be equal to 100.0 mm and 4.0 mm, respectively, for both the holders. Length of thigh link is assumed to be equal to 480.0 mm. Thigh link, shank link and metal belt are interconnected using several pins of 6.0 mm diameter. Those hollow cylindrical braces are cut across the mid-plane of the cylinder, such that they are divided into two parts (refer to Fig. 1(b)). There is a slot on the surface of one part of each brace and a slider is welded on the surface of the other part, such that it can freely slide within the slot to connect two parts of a brace. There are several holes on the outer surface of the slot, where a pin can be inserted to lock the two parts of the brace according to the size of a patient's thigh and shank.

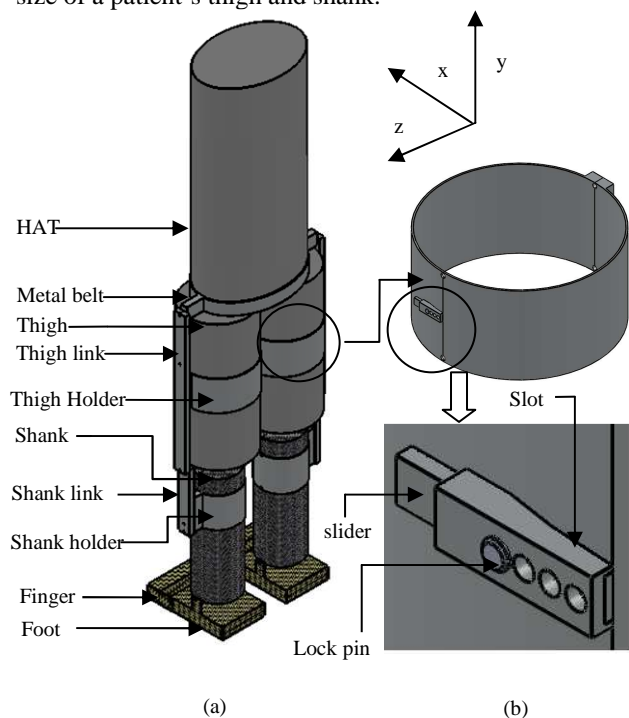


Fig. 1. (Color online) (a) Model of human lower extremity along with body (HAT) and orthotic device without any mechanism (b) zoomed-in view of the slider and slot to show the attachment of the thigh holder with the patient's lower limb.

Lagrangian approach is applied to determine the expression of torque at right and left knee joint with the following assumptions:

- 1) The body moves in x-direction only, without any side-wise movement (i.e., in z-direction).
- 2) It is assumed that ground reaction forces generated by the floor during double support phase are acted on two legs, such that the total load is equally distributed on right and left feet.
- 3) For the analysis of double support phase, the half of mass of the HAT system is considered in order to find out torque and power in both the cases of with and without mechanism.
- 4) Thigh, thigh holder and thigh link are considered to be a single link. Similarly, this assumption is also followed in the case of shank.
- 5) Each of these parts, namely right finger, right foot, right shank, right thigh, HAT (along with metal belt), left thigh, left shank, left foot, left finger is presumed to be a single link in the dynamic modeling.
- 6) Each and every link is assumed to be connected with other link by a revolute joint.
- 7) The lengths of foot, shank, thigh and HAT segments are considered to be equal to 260.0 mm, 430.0 mm, 480.0 mm and 680.0 mm, respectively.
- 8) In the present study, the masses (in Kg) of foot, shank, thigh and HAT are kept equal to 2.6, 10.8, 21.4 and 62.3, respectively.
- 9) The values of moment of inertia (in Kg-mm<sup>2</sup>) for the foot, shank, thigh and HAT are taken as 15978.3, 149180.6, 424249.2 and 2770835.5, respectively.
- 10) The total mass of the model, which represents the human body is taken as 133 Kg approximately.
- 11) The variation of time and different joint parameters like angular displacement, angular velocity and angular acceleration follows the Akima cubic spline developed by Fried and Zietz [12].

Linear displacements of center of mass of *i*-th link along the horizontal and vertical directions are given by (1) and (2):

$$x(i) = \sum_{i=1}^{n(i)} b(i) \cos \sum_{i=1}^{n(i)} \theta(i), \quad (1)$$

$$y(i) = \sum_{i=1}^{n(i)} b(i) \sin \sum_{i=1}^{n(i)} \theta(i), \quad (2)$$

where  $n(i)$  is the total number of links up to *i*-th link. Here, the term  $b(i)$  denotes length of *i*-th link, when  $i \neq n(i)$ , and it denotes distance of center of mass of *i*-th link, when  $i = n(i)$ . It is to be noted here that stance foot (1<sup>st</sup> link) is considered as the starting body for the analysis.

Linear velocity for *i*-th link is given by (3):

$$v(i) = \sqrt{\dot{x}(i)^2 + \dot{y}(i)^2} \quad (3)$$

The kinetic energy  $K(i)$  and potential energy  $P(i)$  for *i*-th link are expressed in (4) and (5):

$$K(i) = \frac{1}{2} m(i) v(i)^2 + \frac{1}{2} I(i) \omega(i)^2, \quad (4)$$

$$P(i) = \frac{1}{2} m(i) g y(i), \quad (5)$$

where  $m(i)$  is the mass of *i*-th link and  $g$  is the acceleration due to gravity.  $I(i)$  denotes moment of inertia (kg-mm<sup>2</sup>) of *i*-th link,  $\dot{x}(i)$  and  $\dot{y}(i)$  are linear velocity of center of mass of *i*-th link along horizontal and vertical directions, respectively.  $\omega(i)$  is angular velocity (rad/s) of *i*-th link.

Lagrangian  $L$  for the whole system and torque  $\tau(i)$  for *i*-th link are expressed by (6) and (7), as given below:

$$L = \sum_{i=1}^n (K(i) - P(i)) \quad (6)$$

$$\tau(i) = \frac{d}{dt} \left( \frac{\partial L}{\partial \dot{\theta}(i)} \right) - \frac{\partial L}{\partial \theta(i)} \quad (7)$$

Putting the expression of  $x(i)$ ,  $y(i)$ ,  $v(i)$ ,  $K(i)$ ,  $P(i)$  and  $L$  into the equation (6), final expression for the torque without mechanism  $\tau_{wom}(i)$  for *i*-th link can be obtained, which, as given in (8):

$$\tau_{wom}(i) = D(\theta(i), \ddot{\theta}(i)) + h(\theta(i), \ddot{\theta}(i)) + C(\theta(i)), \quad (8)$$

where  $D$ ,  $h$  and  $c$  represent inertia, centrifugal and Coriolis and gravity terms, respectively.  $\theta(i)$ ,  $\dot{\theta}(i)$  and  $\ddot{\theta}(i)$  are angular displacement, velocity and acceleration for *i*-th link, respectively.

Power consumption for *i*-th link  $P_{wom}(i)$  is calculated by the following expression, as given below:

$$P_{wom}(i) = \tau_{wom}(i) \dot{\theta}(i) \quad (9)$$

To consider the heat loss of motor, an extra term will be added to obtain the expression for actual power consumption for *i*-th link, as given in (10):

$$P_{wom}(i) = \tau_{wom}(i) \dot{\theta}(i) + \int_0^t K \tau_{wom}(i)^2 dt, \quad (10)$$

where energy loss due to heat emission is denoted by the integral term in (10). Here,  $K$  is a constant, whose value (dependent on the properties of motor) is taken to be equal to 0.025 [13].

### B. Device With Mechanism

In Fig. 2(a) and (b), a torque reducing mechanism is shown. Here, a motor is connected to the pinion shaft. With the rotation of the pinion, the gear will rotate and subsequently, the crank and connecting rod will also rotate to get final rotation of shank link, causing the knee joint to move. A gear ratio of 3:1 is used in this mechanism (the number of teeth of pinion is 18).

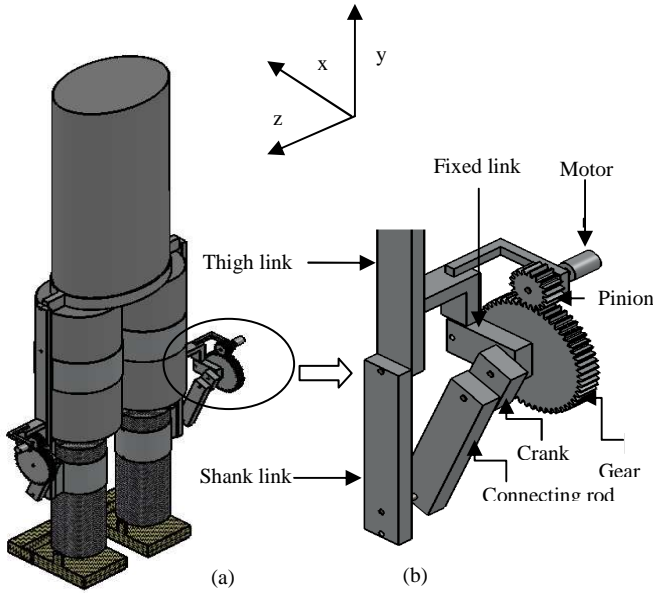


Fig. 2. (Color online) (a) Model of human lower extremity along with body and orthotic device with mechanism (b) zoomed-in view of the mechanism.

For this device with the external mechanism, the torque  $\tau_{wm}(i)$  for  $i$ -th link can be determined as follows:

$$\tau_{wm}(i) = \tau_{wom}(i) \dot{\theta}_{knee}(i) / \dot{\theta}_{pinion}(i), \quad (11)$$

where  $\dot{\theta}_{knee}(i)$  and  $\dot{\theta}_{pinion}(i)$  are angular velocities of knee joint and pinion, respectively for  $i$ -th link. It is also to be noted that power consumption can be determined as discussed above.

### C. Zero Moment Point and Dynamic Balance Margin

The braces with and without mechanism are checked against the dynamic stability of assumed walking pattern. For dynamically balanced walking cycle, the ZMP should not lie outside the sole of supporting foot, known as foot polygon. The friction between foot and ground is assumed to be sufficient to prevent slipping. As no side-wise movement is considered, the ZMP of the system in x-direction is expressed as follows:

$$x_{ZMP} = \frac{\sum_{i=1}^n (I(i)\omega(i) + m(i)x(i)(\ddot{z}(i) - g) - m(i)\ddot{x}(i)z(i))}{\sum_{i=1}^n m(i)(\ddot{z}(i) - g)}, \quad (12)$$

$\ddot{x}(i)$  is the linear acceleration in the direction of walking ( $m/s^2$ ) of  $i$ -th link,  $\ddot{z}(i)$  is the linear acceleration in the z-direction ( $m/s^2$ ) of  $i$ -th link.

Now, to ensure the stability of the system, checking is done whether ZMP lie within the safe zone measured in the direction of movement. Dynamic Balance Margin (DBM) is defined as the distance of the ZMP from the boundary of support polygon. So, the DBM of the system in x-direction is given by the expression:

$$x_{DBM} = \left( \frac{L_{foot}}{2} - |x_{ZMP}| \right) \quad (13)$$

If  $x_{DBM} \leq \frac{L_{foot}}{2}$ , then dynamic stability will be maintained, where  $L_{foot}$  is the length of the foot in contact with floor.

## IV. OPTIMIZATION

For the further reduction of torque at knee joint, optimization is carried out. For optimization, a real coded-GA is used. The design variables are lengths of crank, connecting rod, fixed link and shank link. In real-coded GA, a set of initial population is generated in terms of real number lying within the ranges of design variables. Then, the values of objective function for different values of candidate solution are calculated. A tournament selection is then used for the selection of candidate solutions from the initial population to form the mating pool. By using simulated binary crossover [14], children solutions are formed with the help of crossover probability, which allows the chosen solutions to compete. A polynomial mutation [15] is then utilized to further bring diversification in the solution. It completes one cycle of the GA.

## V. RESULTS AND DISCUSSION

### A. Dynamic Analysis of the Device Without Mechanism

Swing and stance phases of a gait cycle (refer to Fig. 3) of normal walking are considered for the dynamic analysis. The motion starts from the stance phase of right leg, while left leg will start the swing phase. The total cycle time is taken as 8.0 seconds starting from 0 in a time step of 0.04 seconds. Cycle time is taken to be more than that of a normal gait, as motor impaired patients cannot walk with the same speed as that of normal human being. The first half of the cycle, starts with the stance phase of right leg and continues up to the end of swing phase of left leg, having the duration of 4.0 seconds. The second half of the cycle starts with the stance phase of left leg and ends with the swing phase of right leg. The stride length during one cycle is assumed to be equal to 780.0 mm.

Figs. 4 and 5 show the variations of knee joint angle, hip joint angle and ankle joint angle with respect to time for the right and left legs, respectively.

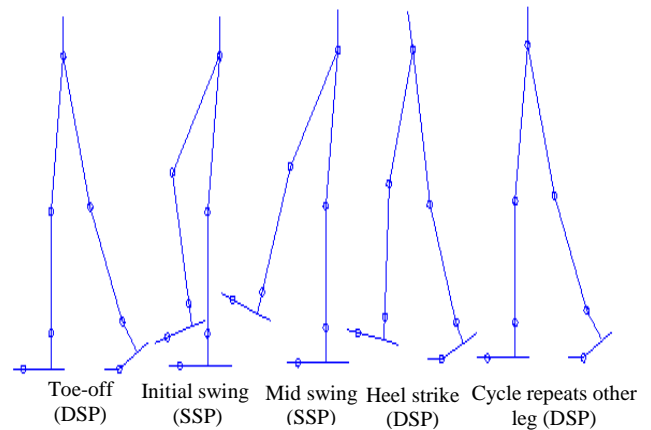


Fig. 3. (Color online) Assumed gait cycle showing single support phase (SSP) and double support phase (DSP).

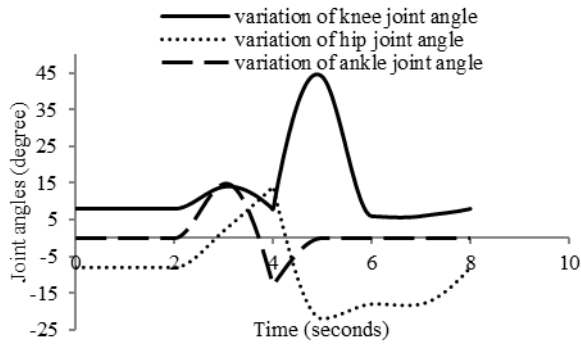


Fig. 4. Plots of joint angles vs. time for right leg.

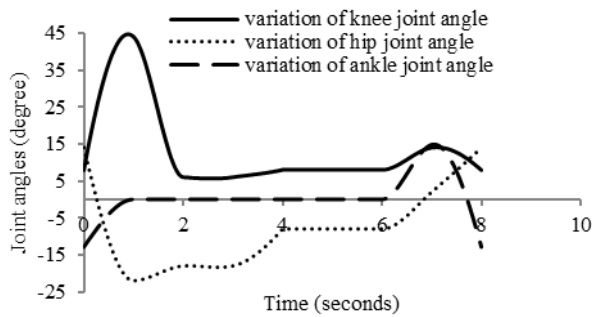


Fig. 5. Plot of joint angles vs. time for left leg.

The variations of torque and power consumption over the cycle time of 8.0 seconds, for the right and left knees are shown in Figs. 6 and 7, and Figs. 8 and 9, respectively.

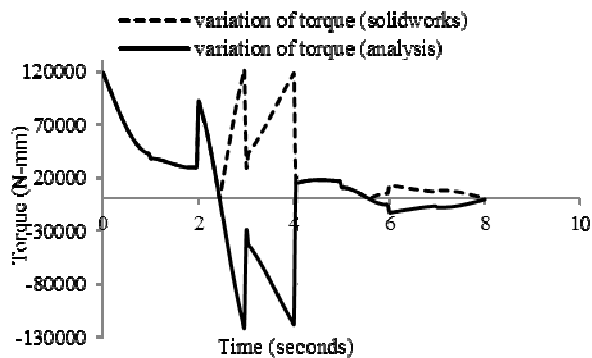


Fig. 6. Plot of torque vs. time at right knee (without mechanism).

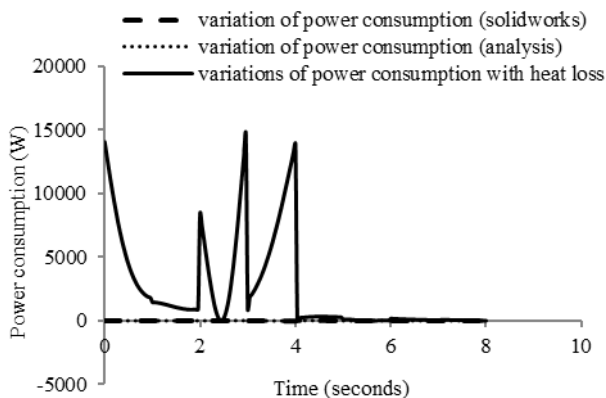


Fig. 7. Plot of power consumption vs. time at right knee (without mechanism).

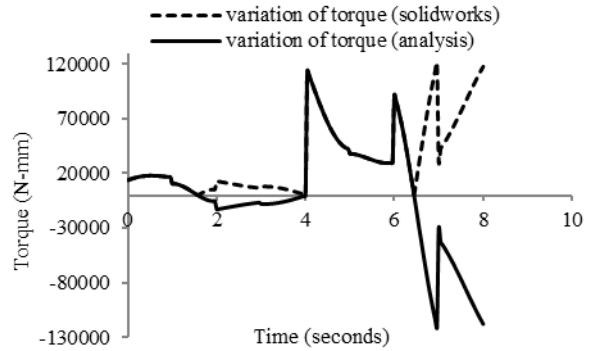


Fig. 8. Plot of torque vs. time at left knee (without mechanism).

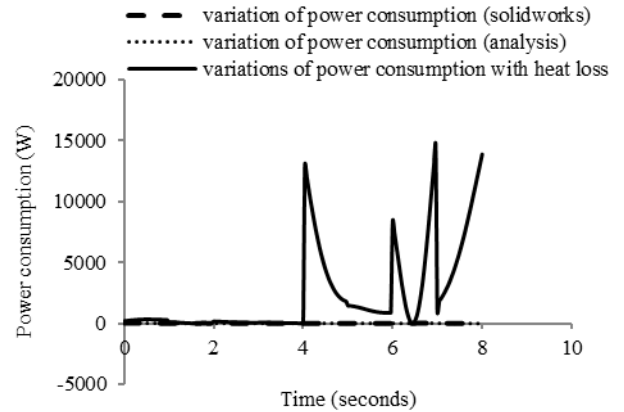


Fig. 9. Plot of power consumption vs. time at left knee (without mechanism).

From Figs. 6 and 7, it is clear that the magnitude of torque and power consumption for right knee, calculated by solid-works and analytical method are almost the same, with an average percent deviation of 0.002067% in case of torque and 0.001969% in case of power consumption. For the left knee, magnitudes of torque and power consumption obtained by the solid-works and analytical method match with an average percent deviation of 0.0020675% and -0.001983%, respectively (refer to Figs. 8 and 9). It is to be noted that solid works show the magnitude of the torque values only. But, knee joint moves both in clock-wise and anti-clockwise directions, which causes the torque values to be negative also, which is shown in the analytical results.

### B. Dynamic Balance of the Device without Mechanism

From (12) and (13), the locus of ZMP and DBM over the gait cycle (0.0 to 8.0 seconds) is determined, as shown in Fig. 10.

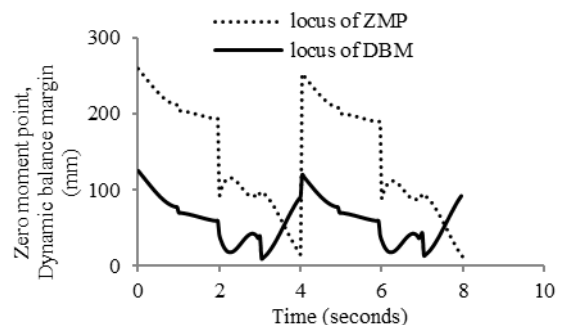


Fig. 10. Plot of ZMP, DBM values vs. time without mechanism.

From Fig. 10, it is clear that during the first half of cycle, all the values of DBM throughout the cycle (maximum value is 125.19 mm) are found to be less than that of  $\frac{L_{foot}}{2}$ , which is equal to 134 mm, during 0.0 to 2.96 seconds, as the whole foot and finger are in contact with the ground. For the time duration of 3.0 to 3.96 seconds, when only fingers are in contact with the ground, the length of contact zone of foot with ground becomes equal to 106.81 mm. During this time period, the maximum value of DBM is 91.05 mm, which is less than the length of contact zone of foot with the ground. For the second half, the same scenario is observed for the other foot, which will be in contact with the ground. As the DBM values are found to be positive, it can be concluded that dynamic stability is maintained throughout the cycle.

### C. Dynamic Analysis of the Device With Mechanism

To reduce the torque, a mechanism is introduced (refer to Fig. 2(b)). The optimal values of lengths of different components of that mechanism are obtained by using a real-coded GA. The GA starts with an initial population of solutions selected at random. The objective function is taken as the maximum torque value (denoted by  $\tau_{wm}(i)$  for  $i$ -th link) obtained during the whole cycle time, for the leg which is in the stance phase in each half of cycle, as this leg experience more torque compared to the leg that is in swing phase. But, there may be some solutions for which the mechanism cannot move. These solutions are called infeasible solutions. For, this valid configuration of mechanism the values of different components of the mechanism (refer to Fig. 11) must follow some constraints, as shown in (13), (14) and (15).

$$d = \sqrt{(s^2 + l^2 - 2sl \cos(\alpha))} \quad (14)$$

$$\cos \theta = \frac{q^2 + d^2 - p^2}{2qd} \quad (15)$$

$$\cos \phi = \frac{p^2 + d^2 - q^2}{2pd} \quad (16)$$

To get valid configurations of the mechanism, the value of objective function for which the mechanism will become invalid, is replaced by a penalty term of high value. Again, to maintain dynamic stability, ZMP must lie within the foot (which is in contact with ground) polygon. So, another penalty term is to be added to the previous term, if the dynamic stability is not maintained.

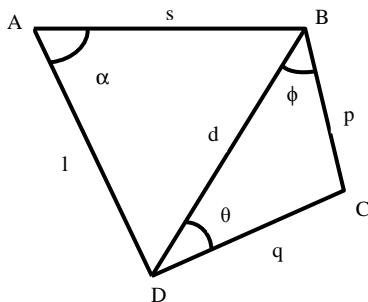


Fig. 11. Schematic diagram of mechanism showing the geometrical configuration

So, the constrained optimization problem may be formulated as follows:

Minimize: maximum value of  $\tau_{wm}(i)$

subject to

$$-1 \leq \frac{q^2 + d^2 - p^2}{2qd} \leq 1,$$

$$-1 \leq \frac{p^2 + d^2 - q^2}{2pd} \leq 1,$$

$$x_{DBM} \leq \frac{L_{foot}}{2},$$

and

$$0 < s < 100, 25 < p < 75, 100 < q < 300, 100 < l < 200,$$

where  $s$  represents the length of fixed link,  $p$  indicates the length of crank,  $q$  denotes the length of connecting rod and  $l$  stands for the length of shank link. Here,  $s$  (denoted by AB in Fig. 11),  $p$  (indicated by BC in Fig. 11),  $q$  (represented by CD in Fig. 11) and  $l$  (represented by DA in Fig. 11) are the decision variables.

Now, a parametric study is carried out to obtain the optimal GA-parameters [16]. In the first stage, by varying crossover probability ( $p_c$ ) from 0.6 to 1.0 in a step of 0.1 and keeping other parameters, such as mutation probability ( $p_m$ ), population size ( $N$ ) and maximum generation ( $G_{max}$ ) fixed at 0.06, 100 and 100, respectively, the minimum torque value is obtained at  $p_c=0.7$ . In the next stage,  $p_m$  is varied from 0.01 to 0.11 in a step of 0.01 after keeping other parameters:  $p_c$ ,  $N$  and  $G_{max}$  fixed at 0.7, 100 and 100, respectively, the minimum value of torque is obtained at  $p_m=0.03$ . Then, in the third stage, by varying  $N$  from 52 to 148 in a step of 8 and keeping other parameters, namely  $p_c$ ,  $p_m$  and  $G_{max}$  fixed at 0.7, 0.03 and 100, respectively, the minimum torque value is obtained at  $N=116$ . In the final stage,  $G_{max}$  is varied from 50 to 150 in a step of 10 and after putting  $p_c=0.7$ ,  $p_m=0.03$  and  $N=116$ , the optimized value of torque is obtained at  $G_{max}=150$ .

The optimal values of decision variables for the minimum value of torque are found to be as follows:  $s=67.82$  mm,  $p=25.41$  mm,  $q=160.55$  mm and  $l=173.14$ mm.

The lengths of different components (namely crank, shank link, connecting rod and fixed link) of the mechanism incorporated in the device are taken to be equal to the values of decision variables obtained through the optimization process.

The variations of torque and power consumption over the cycle time of 8.0 seconds, for the right and left knee are shown in Figs. 12 and 13, and Figs. 14 and 15, respectively, for the device with the geared four-bar mechanism, which are discussed below.

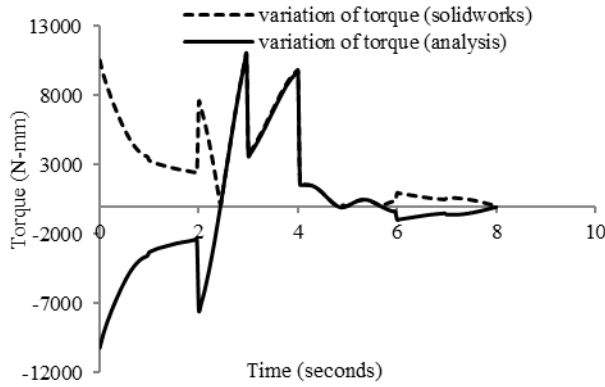


Fig. 12. Plot of torque vs. time at right knee (with mechanism).

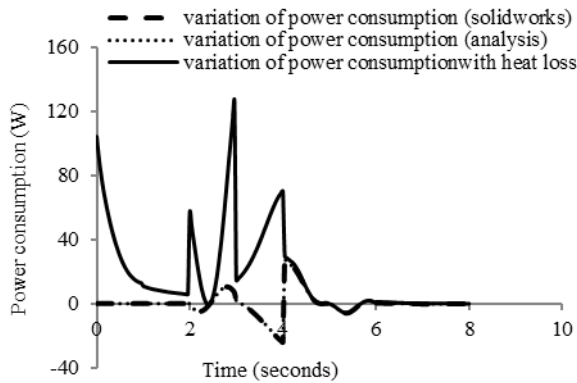


Fig. 13. Plot of power consumption vs. time at right knee (with mechanism).

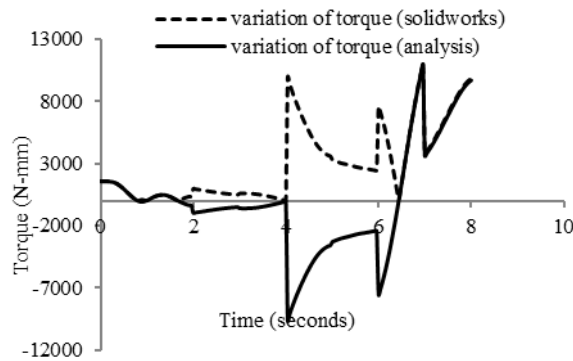


Fig. 14. Plot of torque vs. time at left knee (with mechanism).

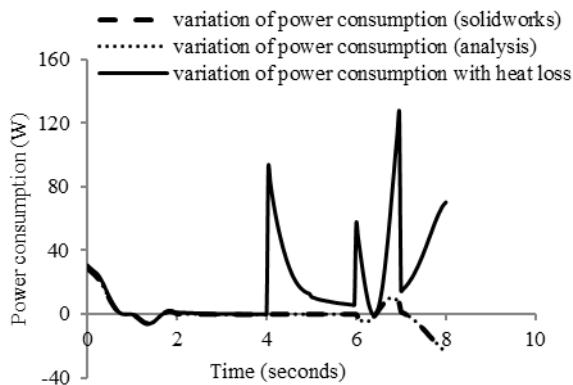


Fig. 15. Plot of power consumption vs. time at left knee (with mechanism).

Figs. 12 and 13 display the variations of torque and power consumption for right knee as obtained by solid-works and analytical approach for the device with mechanism. The values of average percent deviation in predicting the torque and power consumption by the above two approaches are found to be equal to 3.9 % and 4.3 %, respectively. Again, from Figs. 14 and 15, it can be observed that for left knee, the values of torque and power consumption obtained by the solid-works and analytical approach differ by 3.9 % and 4.3 %, respectively.

The average absolute percent (A.A.P.) saving in torque over the gait cycle can be determined as follows:

$$A.A.P. = \frac{1}{m} \sum_{t=1}^m \frac{|\tau_{wom}(t) - \tau_{wm}(t)|}{\tau_{wom}(t)} \times 100\%$$

where m is the total time step, which is kept equal to 201 (0.0 to 8.0 seconds with 0.04 seconds time increment).

For the optimal lengths of different components of the mechanism obtained above, A.A.P. is calculated as 92% by solid-works and 92 % by analytical approach for both the right and left knees. The values of torque and power consumption obtained from solid-works are found to be the same with those yielded by analytical method, in case of the device without mechanism, which provide the whole study a strong ground for verification. In case of device with mechanism, though there are some differences in values of torque and power consumption calculated by the solid-works and analytical method, it is not significant. The reason of these differences may be as follows: solid-works approximates up to two decimal points, whereas in analytical approach, it is taken up to fourth decimal point. To calculate the composite moment of inertia of the links, there are some differences between their calculated values by solid-works and those obtained analytically. In case of real walking, the maximum torque required to move the knee joint is around 54000 N-mm in case of average human being [10]. In this study, the maximum torque (without mechanism) is found to be equal to 118504.81 N-mm, which is larger in comparison to that required for real walking. The reason for this discrepancy is that, in the present study, almost the double mass for each body part has been considered. This torque is found to decrease to 10,530.15 N-mm by attaching the mechanism with the device.

#### D. Dynamic Balance of the Device with Mechanism

Fig. 16 displays the variations of ZMP and DBM with time for the device with the external mechanism.

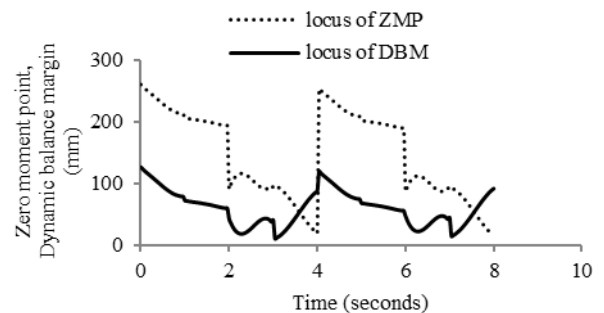


Fig. 16. Plot of ZMP, DBM values vs. time with mechanism.

The nature of variations is found to be similar to that shown in *Fig. 10*. It indicates that dynamic stability is also maintained after attaching the mechanism to the device.

## VI. CONCLUSIONS

The torque required by the device with mechanism to move the knee joint for the assumed gait cycle is considerably reduced in comparison to that of the device without mechanism. Since there is a notable decrease of 92% in torque requirements, the driving unit will require a low capacity motor and consequently, yields a compact, cost effective design. Dynamic stability of the designed orthotic device with the above mechanism has been checked and it is found to be stable and thus, safe for the users. It may, therefore, be concluded that a novel orthotic device has been designed, which can assist the patients in reducing the effort during walking after maintaining the stability of the whole body.

## VII. SCOPE FOR THE FUTURE WORK

Modeling can be made more generalized by varying the angular movement of different parts of lower extremity to obtain different types of gait cycle during normal walking. Side-wise motion may also be included in the analysis. The dynamic study of the device with mechanism may be carried out in order to incorporate more flexibility to the device, in case of staircase ascending and descending. Experimental validation will be done in future by developing a suitable set-up.

## REFERENCES

- [1] B. Dellon, Y. Matsuoka "Prosthetics, Exoskeletons and Rehabilitation-now and future" IEEE Robotics and Automation Magazine, pp. 30-34, March 2007.
- [2] 8th Global Conference on Health Promotion, Finland, June 2013, pp. 10-14.
- [3] <http://en.wikipedia.org/wiki/Prosthesis>, last visited on 18th September, 2013.
- [4] Prosthetics and orthotics-Vocabulary-Part 1: General terms for external limb prostheses and external orthoses- ISO 8549-1:1989.
- [5] D. Bradley, C. A. Marquez, M. Hawley, S. Brownsell, P. Enderby, S. Mawson "NeXOS –The design, development and evaluation of a rehabilitation system for the lower limbs", Mechatronics, In Press.
- [6] M. R. Safizadeh, M. Hussein, M. S. Yaacob, M. Z. Zain, M. R. Abdullah, M. S. CheKob, K. Samat, "Kinematic analysis of powered lower limb orthoses for gait rehabilitation of hemiplegic and hemiparetic patients", Intl. Journal of Mathematical Models and Methods in Applied Sciences, Vol. 5, no. 3, pp. 490-498, 2011.
- [7] Q. Zhang, K. Tian, H. Guo," Development of an Instrumented and Passive Exoskeleton for the Lower Limb Rehabilitation", in Proc. of the Conference of Intl. Association of Computer Science and Information Technology, 2009, pp. 521-525.
- [8] S. K Agrawal., S. K. Banala, A. Fattah., V. Sangwan, V. Krishnamoorthy, J.P. Scholz., and W-L Hsu "Assessment of motion of a swing leg and gait rehabilitation with a gravity balancing exoskeleton" IEEE Trans. on Neural Systems and Rehabilitation Engineering, vol. 15, no. 3, pp. 410-420, September 2007.
- [9] K. Yamamoto, M. Ishii, K. Hyodo, T. Yoshimitsu, and T. Matsuo, "Development of power assisting suit (miniaturization of supply system to realize wearable suit)," JSME Intl. J., Ser. C, vol. 46, no. 3, pp. 923-930, 2003.
- [10] E. D. Lemaire, L. Goudreau, T. Yakimovich, and K. Jonathan - "Angular-velocity control approach for stance-control orthoses" IEEE Trans. on Neural Systems and Rehabilitation Engineering, vol. 17, no. 5, pp. 497-503, October 2009.
- [11] J. Nikitczuk, B. Weinberg, P.K. Canavan, and C. Mavroidis, "Active knee rehabilitation orthotic device with variable damping characteristics implemented via an electrorheological fluid" IEEE Trans. on Neural Systems and Rehabilitation Engineering, vol. 15, no. 6, pp. 952-960, December 2010.
- [12] J. Fried, S. Zietz "Curve fitting by spline and Akima methods: possibility of interpolation error and its Suppression" Physics in Medicine and Biology, vol. 18, no. 4, pp. 550-558, 1973.
- [13] J. Nishii, K. Ogawa, R. Suzuki, "The optimal gait pattern in hexapods based on energetic efficiency," in Proc. of 3<sup>rd</sup> Intl. Symposium on Artificial life and Robotics, Japan 1998, pp. 106-109.
- [14] K. Deb, R.B. Agrawal, "Simulated binary crossover for continuous search space", Complex Systems, vol. 9, no. 2, pp. 115-148, 1995.
- [15] K. Deb, M. Goyal, "A combined genetic adaptive search (GeneAS) for engineering design", Computer Science and Informatics, vol. 26, no. 4, pp. 30-45, 1996.
- [16] D.K. Pratihari, Soft Computing. New Delhi, Narosa Publishing House, 2008.